SHAPE COEXISTENCE, EVOLUTION AND THE PARALLEL PROTON–NEUTRON CORE BREAKING IN $^{155}_{68}Er_{87}$ STUDIED WITH THE HELP OF THE BaF_2 4π-DETECTION SYSTEM

F.A. BECK, T. BYRSKI, S. ROUABAH, D. CURIEN, N. BENDJABALLAH[1], C. COSTA, C. GEHRINGER, B. HAAS, J.C. MERDINGER, J.P. VIVIEN
CRN Strasbourg, F-67037 Strasbourg Cedex, France

G. BASTIN, C. SCHÜCK
CSNSM Orsay, BP 1, F-91406 Orsay, France

D. FREKERS[2], R.V.F. JANSSENS, T.L. KHOO, W. KÜHN[3]
Physics Division, Argonne National Laboratory[4], Argonne, IL 60439, USA

J. DUDEK, F. MENAS and W. NAZAREWICZ[5]
CRN Strasbourg et Université Louis Pasteur, F-67037 Strasbourg Cedex, France

Received 4 February 1987

A discrete γ-ray study of ^{155}Er has been performed. A level scheme up to spin 85/2 has been established and interpreted using the deformed Woods–Saxon cranking approximation, taking into account pairing forces. Interpretation in terms of shape coexistence, band termination and breaking of the ($Z=64$, $N=82$) core is proposed.

The ^{155}Er nucleus belongs to the so-called transitional nuclei in the rare earth region. The special structural features which demonstrate themselves in its decay pattern are determined primarily by a relatively large number of valence particles ($\Delta Z=4$ and $\Delta N=5$ on top of the $Z=64$ and $N=82$ closed shells for protons and neutrons, respectively). The neighbouring ^{156}Er isotone displays a collective-rotational decay pattern at low and moderately high spins which seems to terminate while the nucleus develops an oblate shape at higher spins [1]. Conversely in ^{154}Er a typical non-collective structure has been established [2,3] involving at the highest spins the breaking [3] of the proton or neutron cores. Hence, a study of possible shape coexistence and shape transition effects through the interplay of individual and collective degrees of freedom seems to be particularly challenging for the ^{155}Er nucleus.

Moreover, in the nuclei discussed, a special example of a shape transition, the so-called band termination, may also be expected. In such a case a nucleus undergoes a loss of collectivity while the nuclear shape acquires an axial symmetry with respect to the direction of spin. Realistic calculations indicate [4] that this mechanism is likely to occur in this region for a nuclei with about 8–10 valence particles.

The levels of ^{155}Er were studied by the ^{125}Te(^{34}S, 4n) reaction in two different sets of experiments. A 1 mg/cm^2 95% isotopically enriched ^{125}Te target on a 50 mg/cm^2 lead backing was used. In the first

[1] Permanent address: USTHB, Dar El-Beïda, Algiers, Algeria.
[2] Permanent address: TRIUMF, 4004 Wesbrook Mall, Vancouver, Canada V6T 2A3.
[3] Permanent address: II. Physikalisches Institut, Universität Giessen, D-6300 Giessen, Fed. Rep. Germany.
[4] Work supported by the US Department of Energy under contract No. W-31-109-Enj-38.
[5] Permanent address: Institute of Technology, PL-00-662 Warsaw, Poland.

0370-2693/87/$ 03.50

experiment, performed at the Argonne Tandem-Linac, the experimental set-up included three Ge detectors and two large 25 cm×30 cm NaI crystals used as a sum spectrometer. An excitation function versus bombarding energy was measured between 150 and 170 MeV in steps of 5 MeV and a first γ–γ coincidence experiment at 165 MeV. The subsequent level scheme was tentatively built up to $I=63/2$. A second experiment was performed at the Strasbourg MP tandem by using the 4π BaF_2 "Château de Cristal" array [5] with a 166 MeV ^{34}S beam. In this case 12 Compton-suppressed Ge detectors located at 26 cm from the target and at three different angles relative to the beam direction (four detectors at each of the following angles: $\theta=33°$, 147° and 90°) were placed around a "reduced" version of the "Château de Cristal" including 38 BaF_2 elements. Two additional planar Ge detectors were included in this set-up in order to detect low energy γ-rays. Three types of selection conditions were combined to obtain very clean ^{155}Er spectra. Besides fold and sum-energy recording, the excellent timing performance of the BaF_2 detectors was used to discriminate the 4n from the 5n channel through the delayed γ-rays emitted below the ^{155}Er and ^{154}Er isomers which have approximately the same half-lives ($T_{1/2}\simeq 30$ ns) but differ by their multiplicities. Those multiplicities are 1 and 5 for ^{155}Er and ^{154}Er, respectively. Therefore two types of fold distributions were measured using different simultaneous timing conditions with respect to the first BaF_2 counter which triggered:

– the fold number within 2 ns after the BaF_2 trigger (prompt fold).

– the fold number of γ rays occurring at least 30 ns after the trigger (delayed fold).

The delayed fold number allowed to select on line "quasi singles" spectra corresponding to ^{155}Er nuclei (1 delayed γ-ray). These spectra have been used to determine the γ-anisotropies through the ratio $W(90°)/W(33°)$. Over 6×10^7 coincidence events were recorded out of which the 4n channel represented approximately 50%.

To determine the transition multipolarities we have used the method [2] of simultaneous linear polarisation and angular distribution measurement. This has been done in coincidence with prompt and delayed folds provided by Château. The five Ge polarimeter was placed at $\theta=-90°$ with respect to the beam axis. The angular distribution was measured with six Ge Compton-suppressed detectors, two at each of the following angles: $\theta=12°$, 90° and 147°.

The decay scheme established from the γ–γ coincidence spectra, transition intensities and anisotropies is given in fig. 1. The level scheme of ^{155}Er was previously known [6] up to spin 41/2.

The low spin part of the decay scheme shows a characteristic sequence: the rotational band built on the $I^\pi=13/2^+$ state decaying via the $I^\pi=11/2^-$ excited state to the $I^\pi=7/2^-$ ground state. This type of behaviour is characteristic of many $N=87$ isotones (see for example refs. [7–9] for ^{153}Dy, ^{151}Gd and ^{149}Sm).

Using a self-supporting target and looking for the delayed γ-rays emitted a few centimeters behind the target we found that the $13/2^+$ isomeric state decays via a 31.6 keV transition (cf. fig. 1). The E1-character of this transition was deduced from its intensity relative to the following 531 keV E2 transition. These two transitions have also been observed [10] in the radioactive decay of ^{155}Tm. Thus, the energy of all levels is established firmly. A major problem in the experimental analysis is the connection between the $41/2^+\rightarrow13/2^+$ level sequence and the rest of the decay scheme. The existence of an 85.3 keV transition was established from the energy spectra of the two planar Ge detectors in coincidence with any of the other 12 Ge detectors. The coincidence between the 85.3 keV line and the 640 keV transition is clearly enhanced, even after taking into account the fact that its energy is very close to that of the Pb K_β line and that its intensity is reduced by the internal conversion effect. This result agrees with the long lifetime observed [11] previously ($\tau=1.3$ ns) and supports the interpretation of the $E_x=5013$ keV state as an isomer decaying through the 85.3 keV (M1) and 225 keV (E2) transitions.

The angular distributions and linear polarisations observed for the 344, 405 and 500 keV γ-rays are consistent with the M1+E2 character of those transitions. Therefore spin and parity values for the "sidebands" have been adopted as given in fig. 1. Above 5 MeV excitation energy, two main decay paths include dipole and quadrupole transitions without any strong energy correlation. Around $E_x=11$ MeV the two branches connect again through a 231 keV γ-ray and, may be, through a 669 keV line, the

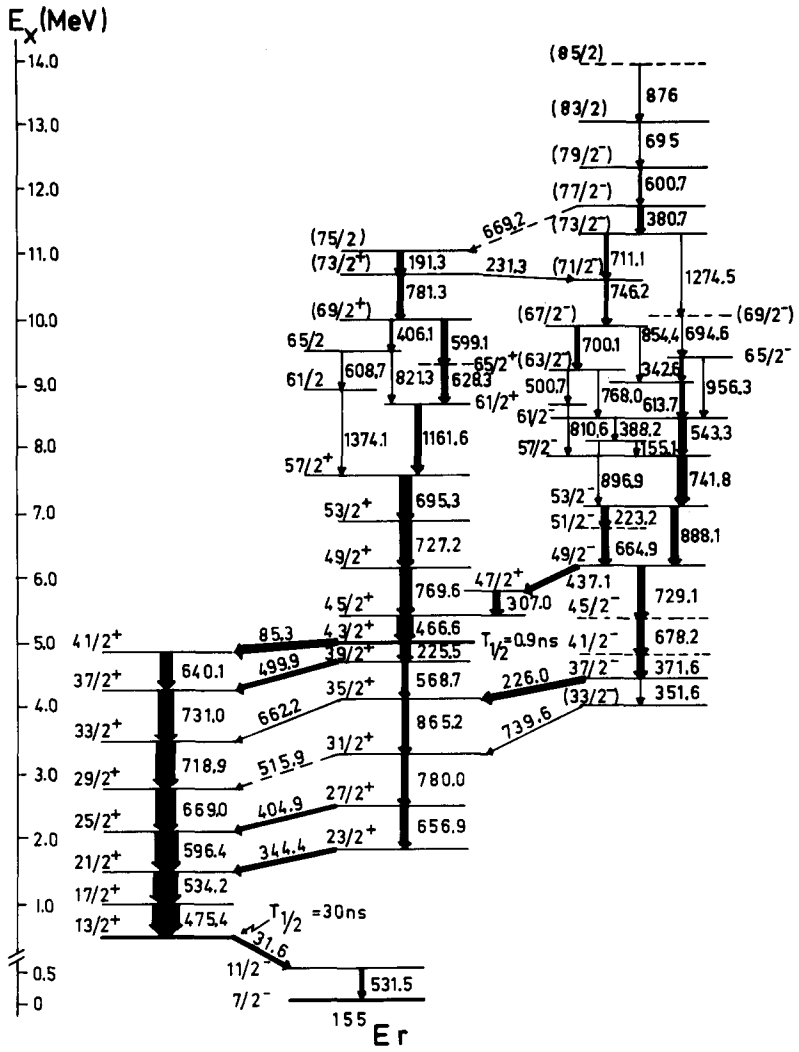

Fig. 1. Partial decay scheme of the ^{155}Er nucleus.

observed scheme ending with a single sequence which extends up to $E_x \simeq 14$ MeV.

From the energy spacings and multipolarities of the transitions in various level sequences of fig. 1, it is clear that the low spin collective character of ^{155}Er terminates at $I \sim 41/2$ thus giving way to a characteristic irregular particle–hole structure, similar to the one observed [9] in the isotone ^{153}Dy.

The non-collective $f_{7/2}$ structure of the ground state and the dominating $i_{13/2}$ character of the rotational band have been pointed out already in ref. [7], where a detailed theoretical analysis was, however, not given. To interpret the foreseen shape coexistence effects we employ the extended Strutinsky procedure [12]. It is based on the hamiltonian

$$H^{\omega} = H + H_{\mathrm{p}} - \omega j_x ,$$

where H and

$$H_{\mathrm{p}} = -G \sum 4 a_n^{+} a_{\bar{n}}^{+} a_{\bar{n}'} a_{n'}$$

denote the Woods–Saxon and the monopole pairing terms, respectively, $(-\omega j_x)$ is the usual "cranking" term and $|\bar{n}\rangle$ refers to the signature-conjugate coupling. In the present calculation we follow the treatment of pairing proposed in refs. [13,14]. In order to perform the calculations effectively over large defor-

mation spaces we simplify the treatment by using the average-pairing approach

$$-G\sum a_n^+ a_{\bar{n}}^+ a_{\bar{n}'} a_{n'}$$

$$= -GP^+P \to -G\tfrac{1}{2}(\langle P^+\rangle P + P^+\langle P\rangle)$$

$$= -\tfrac{1}{2}\Delta(P^+ + P)\,,$$

where

$$P^+ = \sum_n a_n^+ a_{\bar{n}}^+ \,.$$

In the case of rotation the above relation generalises trivially to an analogous one in which one replaces $\Delta \to \Delta(\omega)$. In this way we model the pairing-gap dependence on rotational frequency, $\Delta = \Delta(\omega)$ so that all the important features [13,14] of the self-consistent solutions are preserved, while the numerical treatment is considerably simplified [15].

The total energy surfaces represented in the rotating coordinate system (the routhians) are illustrated in fig. 2. It shows that the ground-state ($7/2^-$) equilibrium deformation corresponds to a nearly spherical-shape configuration ($\beta_2 \simeq 0.05$, $\gamma = 60°$). For $I^\pi = 13/2^+$ and higher, the calculated equilibrium deformation is $\beta_2 \simeq 0.18$, $\gamma \simeq -5°$ giving rise to the collective rotational band (cf. fig. 1). It is worth emphasizing, that taking into account the pairing correlations was essential for obtaining the "collective/non-collective" *shape-coexistence* picture and the correct level sequence; the no-pairing approximation results in a prolate deformed ground-state.

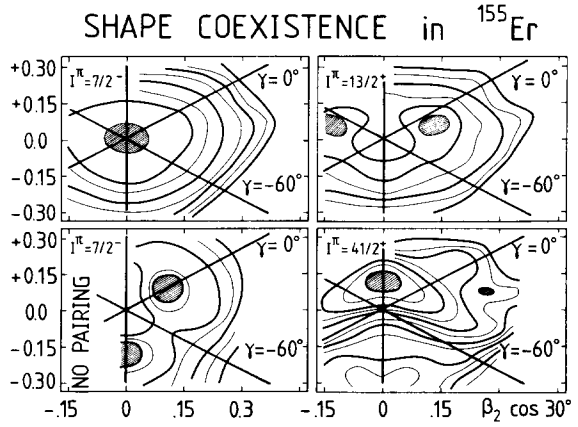

Fig. 2. Results of the theoretical calculations for the total energy surfaces in ^{155}Er. The spherical equilibrium deformation of the ground state ($I^\pi = 7/2^-$) is reproduced only after inclusion of pairing. At $I^\pi = 13/2^+$ collective rotation dominates, but is calculated to terminate in a non-collective, oblate shape configuration at higher spins. For compison a no-pairing calculation result is also given (lower-left frame). We use the parametrisation of the quadrupole deformation in terms of the (β_2, γ) degrees of freedom like the one in ref. [16], eq. (6-90), except that sign convention for the γ-angle is in our case opposite (in our case $\gamma = 60°$ corresponds to non-collective oblate shape configurations). The horizontal axis is not the coordinate axis in the (β_2, γ)-plane but rather its projection and we mark this fact with the symbol "$\beta_2 \cos 30°$".

The band extending from $I^\pi = 13/2^+$ to $I^\pi = 14/2^+$ is predicted to terminate at the latter state which corresponds to $\gamma = 60°$ deformation, fig. 2.

We performed the calculations of the multi-particle multi-hole structure corresponding to the non-collective ($\gamma = 60°$) rotation. We used the approach presented already earlier [17,18]. The results indicate the following global features.

The characteristic isomer at $I^\pi = (43/2^+)$ corresponds most likely to the structure

^{155}Er:

$$\nu(i_{13/2}, h_{9/2})^{max}_{11} \otimes (f^3_{7/2})^{max}_{5/2..} \otimes \pi(h^4_{11/2})^{max}_{8..} \,,$$

analogous to the 19 isomer in ^{154}Er (deexciting via a $E_\gamma = 455.4$ keV transition) whose lifetime [19] is $\tau = 105$ ps and whose proposed [2] structure is

^{154}Er:

$$\nu(i_{13/2}, h_{9/2})^{max}_{11} \otimes (f^2_{7/2})_0 \otimes \pi(h^4_{11/2})^{max}_{8..} \,.$$

Taking into account the transition-energy ratio (455.4/225.5) and the corresponding branching ratio one may estimate an upper limit for the lifetime of the $43/2^+$ isomer of ~ 2 ns as compared to $\tau = 1.3$ ns measured. This relation argues in favour of the interpretation adopted. Here and in the following the double-dot symbol .. refers to the coupling of one pair of nucleons to zero angular momentum (such an effect is a consequence of the monopole-pairing coupling scheme employed here and in the configuration above it applies to the $\pm 7/2$ orbitals in $f_{7/2}$ and $\pm 11/2$ orbitals in $h_{11/2}$). The superscript "max" refers to the maximum alignment within the remaining freedom permitted by the Pauli principle.

Calculations predict a characteristic lowering of energies of the maximum alignment configurations coresponding to spins $43/2^+$ (see above) and the

alternative two $71/2^+$ states. The calculated most probable structures of the latter two states are

$71/2^+$:

$$\nu(i_{13/2}, f^2_{7/2})_{23/2} \otimes (h^2_{9/2})^{max}_8 \otimes \pi(h^4_{11/2})^{max}_{16} ,$$

and

$71/2^+$:

$$\nu(i^2_{13/2})^{max}_{12} \otimes (f^2_{7/2})^{max}_6 \otimes h^{max}_{9/2} \otimes \pi(h^5_{11/2}, d^{-1}_{5/2})^{max}_{13} .$$

Theoretical results suggest therefore that the presence of two complicated decay branches connected by a few transitions only should be related to a presence (absence) of states to which the $\pi(d^{-1}_{5/2})$ contributes, although a direct comparison at this spin range is difficult due to the experimental spin–parity uncertainties.

The sequence $65/2 \rightarrow 61/2 \rightarrow 57/2$ with transition energies 608.7 keV and 1374.1 keV, respectively, resembles very much the sequence $31^- \rightarrow 29^- \rightarrow 27^-$ in ^{154}Er, ref. [2], with the energies 633 keV and 1369 keV, correspondingly. This may be used to support the analogy between the ^{154}Er:

$$\nu(h_{9/2}, i_{13/2})^{max}_{11} \otimes (f^2_{7/2})^{max}_6 \otimes \{\pi(h^4_{11/2})_{16} \rightarrow \pi(h^4_{11/2})_{14} \rightarrow \pi(h^4_{11/2})_{12} \rightarrow \pi(h^4_{11/2})_{10}\}$$

and the ^{155}Er nucleus:

$$\pi(h^2_{9/2}, i_{13/2})^{max}_{29/2} \otimes (f^2_{7/2})^{max}_6 \otimes \{\pi(h^4_{11/2})_{16} \rightarrow \pi(h^4_{11/2})_{14} \rightarrow \pi(h^4_{11/2})_{12} \rightarrow \pi(h^4_{11/2})_{10}\}$$

the latter structures having spins $73/2^+ \rightarrow 69/2^+ \rightarrow 65/2^+ \rightarrow 61/2^+$, respectively.

The maximum angular momentum possible to combine after breaking the proton core (with $(d^{-1}_{5/2})_{5/2}$ state) corresponds to the (yet unobserved) configuration

$89/2^-$:

$$\nu(i^3_{13/2})^{max}_{33/2} \otimes (f_{7/2}, h_{9/2})^{max}_8 \otimes \pi(h^5_{11/2}, d^{-1}_{5/2})^{max}_{20} ,$$

which, according to the theory, feeds the sequence $87/2^+ \rightarrow 85/2^+ \rightarrow 81/2^+ \rightarrow 79/2^-$ with the most likely structures

$87/2^+$:

$$\nu(i^2_{13/2})^{max}_{12} \otimes (h^2_{9/2})^{max}_8 \otimes f_{7/2} \otimes \pi(h^5_{11/2}, d^{-1}_{5/2})^{max}_{20} ,$$

$85/2^+$:

$$\nu(i^2_{13/2})^{max}_{12} \otimes (f^2_{7/2})^{max}_6 \otimes h_{9/2} \otimes \pi(h^5_{11/2}, d^{-1}_{5/2})^{max}_{20} ,$$

$81/2^+$:

$$\nu(i^2_{13/2})^{max}_{12} \otimes (f^2_{7/2})^{max}_6 \otimes h_{9/2} \otimes \pi(h^5_{11/2}, d^{-1}_{5/2})_{18}$$

$79/2^+$:

$$\nu(i^2_{13/2})^{max}_{12} \otimes (h^2_{9/2})^{max}_8 \otimes f_{7/2} \otimes \pi(h^4_{11/2})^{max}_{16} .$$

In summary: We interpret the low part of the decay scheme in terms of a coexistence between slightly oblate and prolate ($\beta_2 \sim 0.18$) equilibrium deformations. The collective band terminates at $I^\pi \sim (41/2^+)$ at the oblate shape ($\gamma = 60°$) configuration. Above that spin the non-collective pattern dominates. Strong equatorial polarisation (of the order of $\beta_2 \simeq 0.16$ to 0.20, $\gamma = 60°$) is predicted by the calculation. The breaking of the proton core is predicted to occur already at $I \sim 53^-$ at the energies very close to the yrast line. Two decay paths in the spectrum are attributed to the configurations involving the proton-core versus neutron-core breaking at the high spins.

Recently a similar feature existing in the $^{150}_{66}Dy_{84}$ nucleus has also been reported [20].

References

[1] F.S. Stephens et al., Phys. Rev. Lett. 54 (1985) 2584.
[2] F.A. Beck et al., Z. Phys. A319 (1984) 119.
[3] C. Schück et al., Proc. XXIII Intern. Meeting on Nuclear physics (Bormio, 1985) p. 294, and to be published.
[4] T. Bengtsson and I. Ragnarsson, Nucl. Phys. A 436 (1985) 14;
I. Ragnarsson et al., Phys. Rev. Lett. 54 (1985) 382.

[5] F.A. Beck, Nuclear Science Research Conference Series, Vol. 7 (Hardwood Academic, New York).
[6] P. Aguer et al., J. Phys. G3 (1977) L1.
[7] P. Kleinheinz et al., Nucl. Phys. A 283 (1977) 189.
[8] J.F.W. Jansen et al., Nucl. Phys. A 321 (1979) 365.
[9] M. Kortelahti et al., Phys. Lett. B 131 (1983) 305.
[10] P. Aguer et al., J. Phys. (Paris) 38 (1977) 435.
[11] R. Kulessa et al., Progress Report GSI Darmstadt (1985); G. Bastin, private communication.
[12] M. de Voigt et al., Rev. Mod. Phys. 55 (1983) 949.
[13] S. Cwiok et al., Phys. Lett. B 76 (1978) 263.
[14] S. Cwiok et al., Nucl. Phys. A 333 (1980) 139.
[15] Lund–Strasbourg–Warsaw Collab., to be published.
[16] A. Bohr and B.R. Mottelson, Nuclear structure, Vol. II (Benjamin, New York, 1975).
[17] G. Andersson et al., Nucl. Phys. A 268 (1976) 205.
[18] J. Dudek et al., Phys. Rev. C 26 (1982) 1712.
[19] P. Aguer et al., Phys. Lett. B 82 (1979) 55.
[20] M.A. Deleplanque et al., to be published.